LA--1624

Copy 15 Of 145

Series A

UNCLASSIFIED

LOS ALAMOS SCIENTIFIC LABORATORY

of the

UNIVERSITY OF CALIFORNIA

PUBLICLY RELEASABLE

Per _Mark Jones_, FSS-16 Date: _10-13-95_

By _Nadine Lujan_, CIC-14 Date: _11-8-95_

LA-1624

This document consists of 44 pages,

Classification changed to UNCLASSIFIED
by authority of the U. S. Atomic Energy Commission,

Per ——— _H. J. Carroll_   _11-7-55_

By REPORT LIBRARY   _V. Martinez_   _11-21-55_

AVERAGE FISSION CROSS SECTION OF U^{238} FOR FISSION NEUTRONS

by

R. B. Leachman and H. W. Schmitt

PHYSICS AND MATHEMATICS

UNCLASSIFIED

UNCLASSIFIED

PHYSICS AND MATHEMATICS

UNCLASSIFIED

ABSTRACT

By means of measurements with a double ionization chamber, the average fission cross section of U^{238} for neutrons from the fission of U^{235} was determined in terms of ν, the average number of neutrons per fission of U^{235}. The number of fissions of U^{238} was measured in one of the ionization chambers while the number of fissions from the fission neutron source of U^{235} was measured in the other chamber. In the nine runs made to determine the cross section, a variety of different methods was used to determine the number of fissions and the mass of U^{238}. The weighted average of these runs gives $\bar{\sigma}_f(28) = (0.756 \pm 0.008)/\nu$ barn or, if the most recent value $\nu = 2.48 \pm 0.03$ is used, $\bar{\sigma}_f(28) = 0.305 \pm 0.005$ barn.

1. Introduction

The average cross section for the fission of U^{238} by neutrons from the fission of U^{235} can be written

$$\bar{\sigma}_f = \int_0^\infty dE_n N(E_n)\sigma_f(E_n), \tag{1}$$

where $\bar{\sigma}_f(E_n)$ is the fission cross section of U^{238} as a function of the neutron energy E_n, and $N(E_n)$ is the probability of a neutron with an energy E_n from the fission of U^{235}. Thus:

$$\int_0^\infty dE_n N(E_n) = 1. \tag{2}$$

Data are available for the calculation of $\bar{\sigma}_f$ from Eq. (1). If $N(E_n)$ as measured by Nereson[1] and Watt[2] is used in Eq. (1) with the $\bar{\sigma}_f(E_n)$ data compiled by Nyer[3] the value $\bar{\sigma}_f = 0.28$ barn is obtained. However, the experimental determinations of $\bar{\sigma}_f(E_n)$ used in this calculation of $\bar{\sigma}_f$ from Eq. (1) involve absolute determinations of neutron flux. Principally because of this, there exists in this method a possibility of significant error in $\bar{\sigma}_f(E_n)$ and, therefore, in this calculated value of $\bar{\sigma}_f$.

The present determination of $\bar{\sigma}_f$ was designed to make use of what seem to be the most reliable data on absolute neutron measurements. To obtain the neutron source strength it was decided to determine the number of fissions in a piece of U^{235}, which served as a fission neutron source. The factor converting the number of U^{235} fissions to the number of fission neutrons is ν. It is believed that the uncertainty in ν is as low as that of any other measurement of neutrons in this energy region. In order to conform with this accuracy of neutron measurement, the present equipment was designed so that the composite of other uncertainties is not greatly in excess of the 1.2 percent uncertainty in ν.[4]

2. Method

Since only the fission neutron source strength Q is determined by observations of the number of U^{235} fissions, it is required of the geometry of the apparatus that the neutron flux nv on the U^{238} be accurately determinable from Q. For this reason, the geometry chosen for the apparatus was hemispherical with the U^{235} neutron source at the center of the hemisphere containing the U^{238}.

Illustrated in Fig. 1 are the essential components of the apparatus, while Fig. 2 is a detailed illustration of the ionization chambers. As can be seen in Fig. 1, thermal neutrons

GRAPHITE

REACTOR SPHERE | BISMUTH

PARAFFIN-FILLED LUCITE BLOCKS

LEAD

BORON-LEAD
BORON

$12\frac{3}{4}$"

$4\frac{1}{4}$"

$\frac{3}{16}$"

12"

18"

8"

12"

24"

24"

$\frac{5}{8}$" 6"

INSULATORS
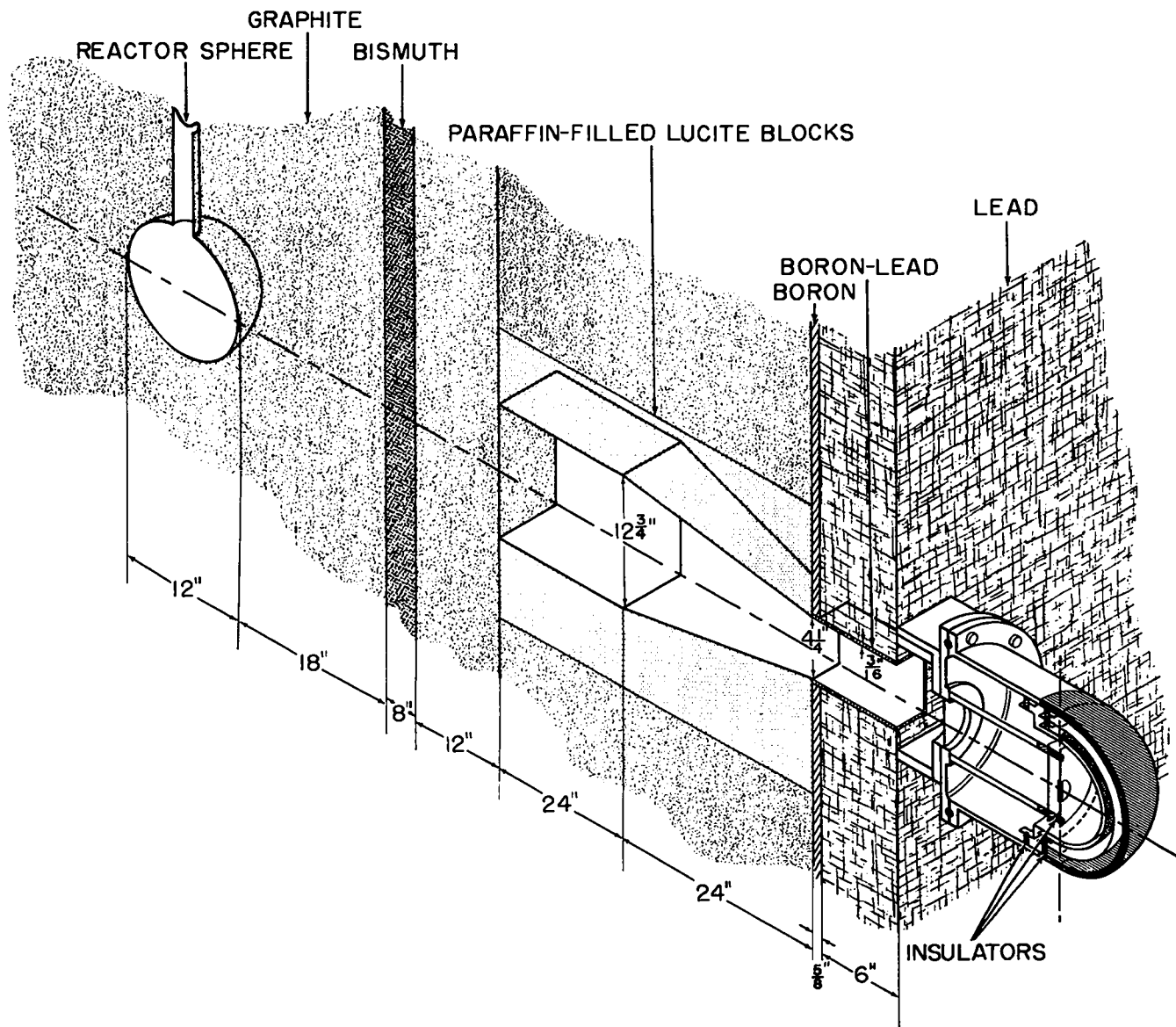
Fig. 1 Cutaway of reactor showing experimental arrangement.

STEEL CYLINDRICAL CASE
COPPER HEMISPHERICAL CASE
U^{238} COATING ON 6"
ALUMINUM HEMISPHERE
MONITOR FOIL
U^{235} DISC SOURCE
5-1/2" CADMIUM SHIELD
9"COLLECTING HEMISPHERE

CONNECTION BOX
PARALLEL PLATE
IONIZATION CHAMBER

U^{235} DISC
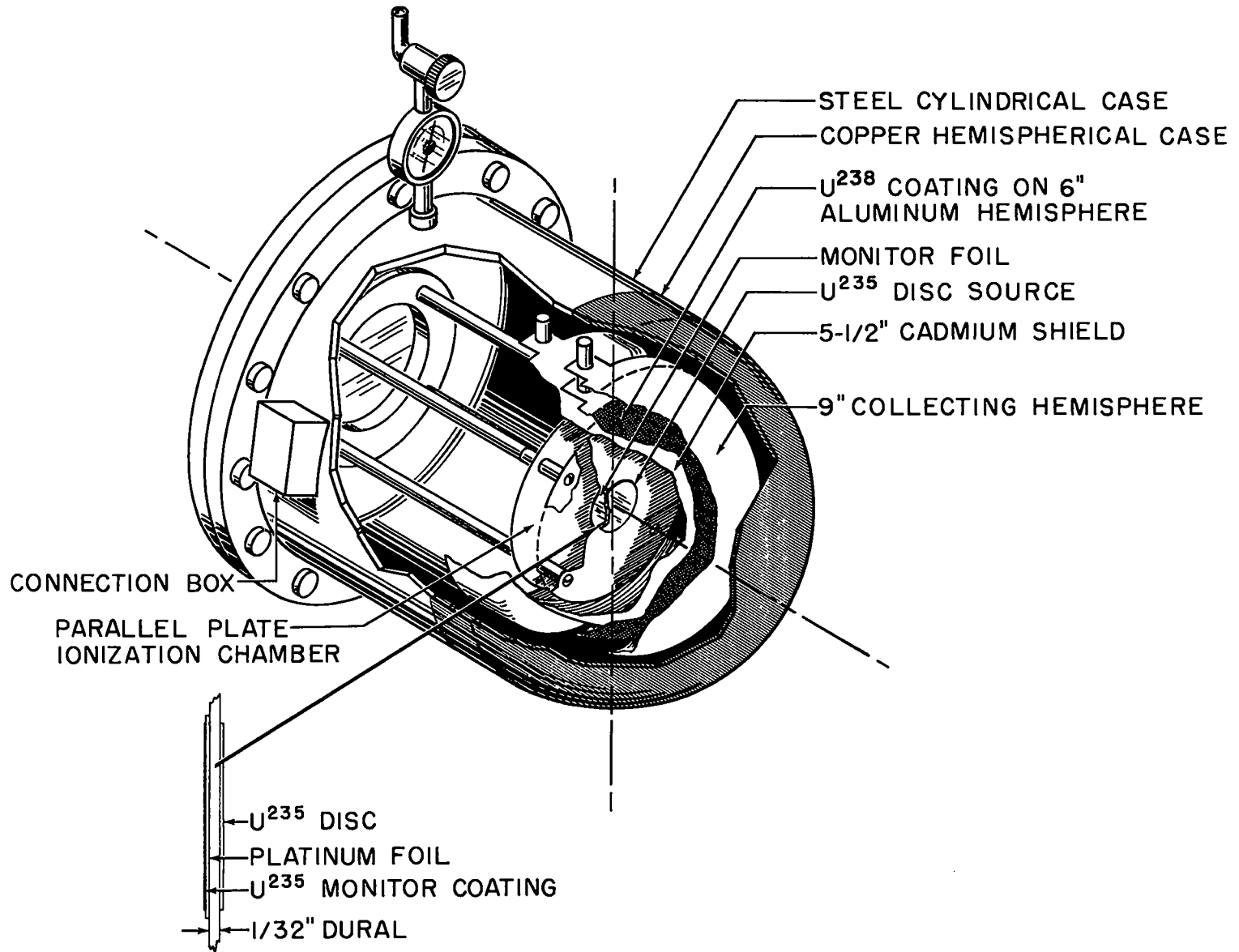PLATINUM FOIL
U^{235} MONITOR COATING
1/32" DURAL

Fig. 2 Detail of double ionization chamber.

to induce fission in the U^{235} neutron source were provided by the Los Alamos Water Boiler reactor. With the thermal column of the reactor as illustrated, the thermal flux upon the U^{235} was $3(10^7)$ neutrons/cm^2/sec. This thermal flux was incident upon a U^{235} metal disc source of 7/8 in. diameter. As seen in Appendix I, the effective flux from the disc source on the U^{238} deposit is only about 1 percent greater than that from a point source of the same Q placed at the center of the hemisphere. Similarly, it can be shown (Appendix II) that extreme nonuniformities in the thickness of the U^{238} deposit lead to corrections that are negligible. If the fission neutron source were a point, the cross section would be determined by

$$N_{28} = \frac{\nu N_{25} \, M_{28} \, (6.023) \, (10^{23}) \, \bar{\sigma}_f}{4\pi r^2 \, (238)} , \tag{3}$$

where N_{28} and N_{25} are the number of fissions in the U^{238} and U^{235}, respectively, r is the radius of the hemisphere in centimeters, and M_{28} is the mass of U^{238} in grams. With the disc source, we have

$$N_{28} = \frac{(6.023) \, (10^{23})}{4\pi \, (238)} \, M_{28} \, N_{25} \, \nu \, \bar{\sigma}_f \, \frac{1}{a^2} \left[\frac{a}{r} \, \ln\left(\frac{r+a}{r-a}\right) + \ln\left(\frac{r^2-a^2}{r^2}\right) \right], \tag{4}$$

where a is the radius of the disc source in centimeters.

Shown in Fig. 2 are the details of the chamber used to determine the quantities N_{25} and N_{28}. The U^{238} in the form of $U_3^{238}O_8$ of 110,000:1 isotopic abundance was on a thin aluminum hemisphere which was concentric with another thin but larger aluminum hemisphere. The two aluminum hemispheres constitute an ionization chamber which detects the U^{238} fission fragments. Cylindrical extensions spun on the hemispheres made possible detection of all fissions. The U^{238} was confined to the hemisphere itself.

To reduce the thermal neutron fission of the U^{235} present in the U^{238}, cadmium shields were placed between the source of thermal neutrons and the hemisphere containing U^{238}. These shields, however, did not eliminate the background fission rate in the hemispherical chamber. Therefore it was necessary to measure the background by removing the U^{235} source and counting only the fissions induced (a) by the gamma rays from the reactor and from neutron capture in the equipment, (b) by fast neutrons from the reactor, and (c) by thermal, leakage neutrons on the U^{235} present in the U^{238} deposit.

As seen in Fig. 2, the disc source, cut from rolled U^{235} metal of either 94.12 or 93.26
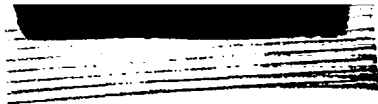
percent isotopic abundance, * was attached to the center of a 1/32 in. thick, 4 in. diameter dural plate and was mounted in a position concentric with the hemispherical chamber. On the other side of the dural plate and mounted just opposite the U^{235} source was a thin monitor foil consisting of thin platinum on which was deposited a known mass M_{25m} of U^{235} in the same diameter as the source. The thinnest deposit used in the monitor in these measurements was about 0.1 μg, while the heaviest used was about 200 μg. The thinnest source used was about 0.001 in. thick and the thickest used was about 0.008 in. thick with masses M_{25} of 0.21 gm and 1.46 gm, respectively. Since the masses of both the U^{235} disc and the U^{235} monitor deposit were known, the number of fissions in the monitor was used in one determination of the total number of U^{235} fissions in each disc source. The fission fragments from the monitor were observed in the ionization chamber formed by the dural plate mentioned above and a similar dural plate parallel to it.

Since the attenuation of the thermal neutrons in the disc sources was appreciable, a correction was necessary. Measurements to determine this correction to better than 1 percent accuracy were made in a parallel-plate, double ionization chamber. Such accuracy was achieved by counting fissions from two thin monitor foils of unknown amounts of U^{235} in the two chambers. These monitor films on platinum, which was black to fragments, sandwiched the U^{235} metal discs being measured. Two sets of counts were used, the direction of the neutron beam being perpendicular to the foils but opposite in direction for the two sets; thus knowledge of the monitor foil masses was unnecessary.

In these measurements of $\bar{\sigma}_f(28)$ an effort was made to have multiple, independent determinations of the quantities in Eq. (4) wherever feasible. The mass of the U^{238} deposit[5] on each of the three aluminum hemispheres used for the various runs was determined by:

(a) The mass difference between the aluminum hemispheres with and without the $U_3^{238}O_8$ deposit;

(b) The rate of alpha-decay of the U^{238}; and

(c) A colorimetric analysis[6] of the uranium on the hemispheres.

In several runs, the number of U^{235} fissions in the source was determined by a radio-chemical analysis[7] of the Mo^{99} content of the bombarded U^{235} disc. In every run, the number of U^{235} fissions in the disc was determined from the number of fission fragments detected by the parallel plate ionization chamber and the relative masses of U^{235} in the monitor and disc

---

*After the measurements had been completed and the U^{235} metal had been reprocessed, it was learned that the pieces of metal used were of either 93.26 or 94.12 percent abundance. Unfortunately, the inventory of these metal pieces was not in good order, and while it is almost certain that the metal pieces used were of 93.26 percent abundance, there exists the possibility that some were of 94.12 percent. The value used in the calculated results is 93.26 percent.
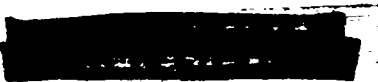
source. The mass M_{25m} of the U^{235} content of the monitor was determined by one or more of the following methods:

(a) Fission counting of the U^{235} deposit in comparison[7] with a standard U^{235} deposit;

(b) The mass difference between the platinum foils with and without the $U_3^{235}O_8$ deposit; and/or

(c) A colorimetric analysis of the uranium on the platinum foil.

Since the standard U^{235} deposits used in (a) amounted to roughly 0.1 μg, this method is most satisfactory for U^{235} deposits of about 1 μg or less. On the other hand, methods (b) and (c) require deposits of 100 μg or greater for 1 percent accuracy. Thus, small deposits were measured only by method (a), and larger deposits only by methods (b) and (c).

The numbers of observed fission fragments from the U^{235} monitor in the parallel plate ionization chamber and from the U^{238} deposit in the hemispherical ionization chamber were recorded by standard Los Alamos electronic equipment. Potentials of roughly 200 volts supplied by batteries were applied across both chambers. The pulses from each chamber were fed to two standard Model 101-A amplifiers and the output from each of these went to a standard Model 700 or 700-A scaler. This provision of duplicate amplifiers and scalers for each chamber made possible an easier detection of malfunctioning electronic equipment. Background fission counts from possible uranium contamination of the chamber components were minimized by having the U^{235} plate, and U^{238} hemisphere, and the cadmium shield all at the same negative potential, while the collecting plate and hemisphere were near ground potential.

3. Results

Several corrections of several percent or less for neutron absorption and neutron scattering must be applied to Eq. (4). Corrections are necessary for absorption and scattering of thermal neutrons in the platinum and dural between the U^{235} deposit and the U^{235} disc. Equation (4) involves only the direct flux of fission neutrons from the U^{235} disc to the U^{238} deposit. Corrections are necessary because fission neutrons were, in addition, scattered to the U^{238} by the reactor face (Appendix III), the outside case of the chamber, and the various hemispheres within the case (Appendix IV). In addition, the absorption of the fission neutrons by the cadmium and the inner aluminum hemisphere was taken into account. The largest of these corrections is 2 to 3 percent for the scattering of neutrons from the hemisphere containing U^{238}; that is, a greater effective thickness of U^{238} is "seen" by the deflected fission neutrons than is "seen" by the unscattered neutrons. Expressions for this correction are developed and applied in Appendix IV.

In order to test qualitatively the validity of this scattering calculation, two different

thicknesses of aluminum hemisphere were used in the cross section measurements. The re-
sults, as seen in Tables 1 and 2, indicate that an error in these calculations of as much as
several percent change in cross section is very unlikely. A measurement of the increase in
the number of U^{238} fissions due to the fission neutrons back-scattered from the copper and
steel outside case of the ionization chamber was made by comparing the number of U^{238}
fissions when a double thickness of steel and copper was used with the number obtained when
the original thickness was used. The percentage increase measured was 0.53 ± 0.3, while,
as shown in Appendix IV, the calculated increase due to the neutrons back-scattered from the
steel and copper was 0.51 percent.

In the various runs, the ionization chamber was filled to 6 ± 1 lb gauge pressure of
tank argon. This pressure caused a bulging outwards of the dural base plate of the ionization
chamber and, as can be pictured from Fig. 2, the U^{235} disc is displaced from the center of
the hemispheres. The amount of the displacement was 0.018 in. and this caused a calculated
0.6 percent decrease in the average fission neutron flux on the U^{238} compared with the flux
from a centered source.

It was expected that the removal of the U^{235} disc would reduce the background by the
amount of the U^{238} photo fissions from the U^{235} fission gamma rays. On the other hand, the
background would be increased by the increase of the thermal flux on the cadmium giving rise
to an increased number of capture gamma rays and leakage neutrons on the U^{238} and its U^{235}
impurity. To determine the validity of the measured backgrounds, tests were made qualitatively
to determine these effects. Gold or aluminum-boron, both of the same opacity to thermal
neutrons as a U^{235} disc, was substituted for the U^{235} disc. Aluminum-boron has capture
gamma rays of 0.51 Mev, whereas gold has capture gamma rays of about 8 Mev. The photo
fission threshold energy is about 6 Mev. Since essentially all fission gamma-ray energies are
less than 5 Mev,[8] it would be expected that the true background with the U^{235} disc present
would be quantitatively between that with the gold and that with the aluminum-boron. The runs
made showed that the background with the gold disc in the position of the U^{235} disc was 1.0 ±
0.5 percent greater than with no disc. Similarly, the background with the aluminum-boron disc
was 0.3 ± 0.5 percent less than with no disc. These results indicate that the backgrounds with
and without the U^{235} disc are the same within the accuracy of the whole experiment. Since the
background U^{238} fissions are always less numerous than the U^{238} fissions induced by fission
neutrons, the uncertainties in the former are less important than in the latter.

Having determined the neutron scattering and absorption corrections to Eq. (4), we now
consider the determination of the quantities N_{25}, N_{28}, and M_{28}, quantities which in this ex-
periment vary from run to run. As mentioned in the previous section, except for the three
Mo^{99} analyses, the quantity N_{25} is determined from

$$N_{25} = (N_{25m} M_{25} T_{25} T_d)/M_{25m}, \tag{5}$$

where in Eq. (5) N_{25} and N_{25m} are the numbers of fissions in the U^{235} disc and monitor, respectively. The effective transmission T_{25} is the average transmission of thermal neutrons into all depths of the U^{235} disc as calculated from the total absorption measurements described in the previous section. The transmission T_d is the transmission of thermal neutrons through the dural plate of the parallel-plate ionization chamber. Thus, in these determinations of N_{25} the quantities N_{25m}, M_{25}, M_{25m}, T_{25}, and T_d must be considered. The transmission T_d is near unity and is calculated in Appendix V.

The number of fissions N_{25m} and N_{28} is determined from linear extrapolations to zero of the integral bias curves obtained from the respective ionization chambers. To this extrapolated number of fissions is added the <1 percent of the fission fragments stopped in the U_3O_8 coatings, as calculated in Appendix VI. Included in Table 1 are the plateau corrections applied to the number of fissions observed in the ionization chambers at the fixed bias used during the runs. The variation of plateau corrections is mainly due to the different gas fillings of the chamber.

The most accurate determination of the quantities under consideration seemed to be that of the mass M_{28} of the U^{238} deposits. The mass M_{28} was first determined by the mass difference between the painted and unpainted aluminum hemispheres. However, since the aluminum hemispheres could only be heated to about $300^{\circ}C$, the uranium nitrate probably was not completely converted to the oxide so that the masses obtained could be used only in a relative sense. For this reason, the weights were used only for a qualitative check on the other determinations.

When the hemisphere with the U^{238} deposit was mounted in the ionization chamber, the alpha-decay rate was measured as a determination of M_{28}. This alpha counting is essentially in 2π geometry and corrections were necessary for the loss of alpha particles in the U^{238} and for back-scattering[9] of alpha particles from the aluminum backing. The U^{238} alpha-decay half-life applicable for this type of measurement was determined by a carefully controlled series of measurements. In these measurements foils of which two independent determinations (colorimetric and weighing after heating to $800^{\circ}C$) of the mass of the 100,000:1 U^{238} were made were alpha-counted in 2π geometry. The alpha-decay half-life was so measured to be $4.56_1(10^9)$ years, which is in excellent agreement with the half-life calculated from the U^{234} half-life and the U^{234}/U^{238} abundance ratio of natural uranium as given by Fleming et al.[10] However, it is in poor agreement with the directly measured value $(4.49 \pm 0.01)(10^9)$ years.[11] Although on the basis of the present careful measurements it is believed the latter half-life value is in error, these measurements were not primarily intended to be an absolute

TABLE 1

RESULTS OF CROSS SECTION RUNS

Run Number	Hemisphere Number	Monitor Foil Number	Disc Source			Plateau Corrections		$\bar{\sigma}_f$ (barns)	Weight of Run (see Text)	Comments
			Nominal Thickness (in.)	U^{235} Mass (gm)	Effective Transmission	N_{25m} (%)	N_{28} (%)			
1	II	1	0.003	0.544	0.8819	4.5	5.0	0.3016	$\sqrt{2}$	
2	II	1	0.002	0.370	0.9187	4.5	5.0	0.3053	$\sqrt{2}$	
3	II	1	0.006	1.039	0.8044	4.0	6.0	0.3022	$\sqrt{2}$	
4	II	2	0.006	1.039	0.8044	0.8	1.7	0.2941	1	Background from U^{235} contamination was 1.6% of N_{25m}
5	II	3	0.003	0.537	0.8835	2.0	2.0	0.2971	1	Input resolution time of scaler results in 0.45% loss in N_{25m}.
6	II	4	0.008	1.363	0.7689	1.0	1.5	0.3064	$\sqrt{3}$	
7	II	5	0.001	0.192	0.9532	1.0	1.5	0.3861	0	Background run known to be in error.
8	I	5	0.006	1.039	0.8044	1.0	1.0	0.3248	1	
9	III	6	0.008	1.360	0.7689	0.7	1.4	0.3091	1	

Weighted average   0.3049 barn (for ν = 2.48)

determination. Instead, because of uncertainties in the back-scattering and alpha-absorption corrections, they gave a quantity applicable to the hemisphere measurements in question.

After use in the cross section experiment, the uranium deposits on the aluminum hemispheres were determined quantitatively by the colorimetric method. Except for the case of one gross, unexplained error, the agreement between colorimetric and alpha-particle determinations was within 0.1 percent.

Aside from the uncertainty in the value of ν, probably the greatest uncertainty involved in the present measurements is in the measurements of N_{25}. The direct determination by Mo^{99} analysis has an accuracy of $\pm$ 5 percent or better. In the present experiment, the results of the Mo^{99} analysis were corrected for the calculated number of Mo^{99} atoms that escaped from the discs as fission fragments. The major uncertainty in N_{25} as determined from Eq. (5) is in the monitor mass M_{25m}. Comparison fission counting of the monitor foils suffered from the disadvantage that the foils in question underwent at least two mountings, one in the comparison chamber and the other in the fission chamber. There was, therefore, the possibility of contamination and crinkling of the foil. In addition, in the comparison fission counting the integral bias curve of the thin standard deposit had less slope that that of the unknown, which generally had a thicker deposit on a less smooth foil. These slopes produced a small uncertainty.

When colorimetric and weighing analyses were used to determine M_{25m}, a compromise between the following considerations was required: (a) a large M_{25m} for accurate mass determination, and (b) a small M_{25m} for a fission counting rate compatible with the resolving time of the electronic equipment. As a result, the 74- to 175-μg monitor masses used were near the lower limit of the weighing and colorimetric methods of analysis. Controlled tests with other foils showed a reproducibility of about $\pm$ 2 μg in weighing after repeated heatings to $800^{o}C$, which converted the uranium to U_3O_8. For these monitor masses the accuracy of the colorimetry method is 2 to 3 percent, whereas for the 46- to 60- mg masses on the hemispheres the 95-percent confidence interval is $\pm$ 0.5 percent.

Table 1 is a summary of the results of this experiment including the corrections listed in the previous sections. The characteristics of the U^{238} deposits and the U^{235} monitor foils are contained in Tables 2 and 3, respectively. As can be seen in Table 2, the agreement between the alpha-counting and colorimetric analyses for hemispheres I and II was excellent. The weight determination was roughly 7 percent high in these cases and also in other test cases. The weight determination in the case of hemisphere III indicates that the U^{238} mass determined by colorimetry is correct and that the mass determined by alpha counting is in error. The reason for this error was not discovered.
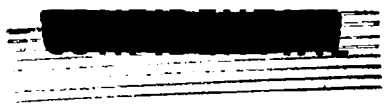
TABLE 2

CHARACTERISTICS OF THE U^{238} HEMISPHERES

Mass determinations by the various methods are given. The fissions from scattering are the calculated percentage of the total U^{238} fissions induced by fission neutrons scattered from the aluminum backing of the hemispheres. The effective scattering thickness is the average thickness of the aluminum hemisphere.

Hemisphere Number	Effective Scattering Thickness (in.)	Fissions from Scattering (%)	U^{238} Mass by Colorimetry (mg)	U^{238} Mass by Alpha-Counting (mg)	U^{238} Mass by Weighing (mg)
I	0.022	2.27	60.6	60.6_8	64.9
II	0.022	2.27	65.6	65.5_8	69.5
III	0.038	3.47	46.6	50.3_5	50.2

4. Conclusions

It is evident that the quantity having the largest uncertainty in these measurements is M_{25m}. Consequently, to determine the best value of $\bar{\sigma}_f(28)$, the values of $\bar{\sigma}_f$ from each individual run were weighted according to the number of independent determinations of M_{25m}. We have rather arbitrarily assigned the same uncertainty to each method of determination. As a result, the weighting of runs relative to those of one determination of M_{25m} is $\sqrt{2}$ for two determinations and $\sqrt{3}$ for three determinations. Thus, runs 4, 5, and 8 had a weight of 1; runs 1, 2, and 3 a weight of $\sqrt{2}$; and run 6 a weight of $\sqrt{3}$. Run 7 was omitted in the calculation of a weighted average because of an uncertainty in its background run.

With such a combination of the results listed in Table 1, the best value is $\bar{\sigma}_f(28) = \dfrac{0.756 \pm 0.008}{\nu}$ barn, where the uncertainty is the standard deviation of the mean. If we use the latest value[4] $\nu = 2.48 \pm 0.03$, where the meaning of the uncertainty is not clear, we obtain $\bar{\sigma}_f(28) = 0.305 \pm 0.005$ barn.

The present value of $\bar{\sigma}_f(28)$ is significantly larger than the 0.28 barn from the reported data and Eq. (1), but the difference is probably not larger than the uncertainty in the values of $\bar{\sigma}_f(E_n)$ used. In contrast, a more recent calculation of $\bar{\sigma}_f(28)$ from Eq. (1), made by Beyster[12] from the recent measurements of $\bar{\sigma}_f(E_n)$ by Henkel and Jarvis, yields $\bar{\sigma}_f(28) = 0.314$ barn. Again, this calculated cross section is of uncertain accuracy principally because of the difficulties associated with absolute flux measurements.
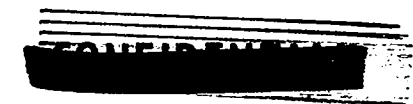
- 14 -

- 15 -

TABLE 3

CHARACTERISTICS AND MEASUREMENTS OF U^{235} MONITOR FOILS

Foil Number	Method of Preparation	Thickness of Platinum Backing (in.)	U^{235} Mass by Weighing (μg)	U^{235} Mass by Colorimetry (μg)	U^{235} Mass by Comparison Fission Counting (μg)	U^{235} Mass Calculated from Mo^{99} Analysis (μg)	Accepted Value of U^{235} Mass (μg)	Number of Determinations Averaged for Accepted Value	Comments
1	Painting	0.002			0.760	0.686 from trial 1. 0.747 from trial 2.	0.763_5	2	Mo^{99} analysis of trial 1 rejected as a gross error. Mo^{99} analysis of trial 1 includes a 3.0% escape probability; 4.3% for trial 2. Plateau in comparison counting was 2.8%, compared with 0.5% for standard foil.
2	Painting	0.002			1.226		1.226	1	Plateau in comparison counting was 2.5%, compared with 0.5% for standard foil.
3	Electro-deposition	0.005			0.0845		0.0845	1	Plateaus of comparison counting were assumed to be the same because of similar foil thickness and because of optimum conditions of mounting. Quantitative electrodeposition was not attempted. Mo^{99} analysis includes 1.2% escape probability.
4	Painting	0.0035	$171._3$	$171._5$		$176._4$	$173._1$	3	
5	Painting	0.0035	$89._1$	$73._7$			$73._7$	1	On the basis of the results of the cross section runs, it is concluded that there is a gross error in the weighing.
6	Painting	0.0035	$127._2$	$153._1$			$127._2$	1	Because of a known failure in the colorimetric analysis, the accuracy of that determination is $\pm$ 20% and so is not used.
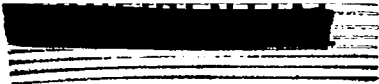
Although it is perhaps misleading, it is interesting to list the incidence of gross errors in the uranium deposit determinations by the various methods used. A gross error is considered to be an error of 5 percent or over. The weighing determinations of M_{28} on the hemispheres was not intended to be a precision measurement and so is not included in Table 4. It should be emphasized that the statistics of the reliability of any one method is poor. Further, it should be pointed out that for the one error of the colorimetry method a mistake had been made in the procedure and, as a result, a ± 20 percent accuracy was placed on the value. In all other cases of gross error, there was no indication of possible error.

TABLE 4

RELIABILITY OF URANIUM MASS DETERMINATIONS

Method	Number of uses		Number of Gross Errors	Approximate Magnitude of the Gross Error (%)	Reliability in This Experiment (%)
	For M_{25m}	For M_{28}			
Mo^{99}	3	0	1	16	67
Comparison fission counting	3	0	0	0	100
Weighing	3	0	1	21	67
Colorimetry	3	3	1	20	83
Alpha counting	0	3	1	8	67

Composite reliability = 78%

5. References

1. N. Nereson, Phys. Rev. **85**, 600 (1952).

2. B. E. Watt, Phys. Rev. **87**, 1037 (1952).

3. W. E. Nyer, LA-994 (1949). The $\sigma_f(E_n)$ used in the present calculation is that of page 14 of LA-994.

4. Harvey and Hughes, BNL-221 (January 1953).

5. In each case the U^{238} was deposited from $U^{238}O_2(NO_3)_2(6H_2O)$ by painting with an alcohol solution. The hemisphere was then heated in an oven to convert the nitrate to $U_3^{238}O_8$.

6. A. L. Henicksman, LA-1394 (March 1952).

7. William Rubinson, LA-613 (November 1946).

8. J. W. Motz, Phys. Rev. **86**, 753 (1952).

9. J. A. Crawford, AECD-2034.
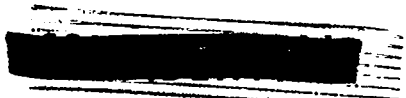
10. Fleming, Ghiorso, and Cunningham, Phys. Rev. **88**, 642 (1952).

11. C. A. Kienberger, Phys. Rev. **76**, 1561 (1949).

12. J. R. Beyster, private communication.

APPENDIX I
DERIVATION OF CROSS SECTION EQUATION (EQ. (4) IN TEXT)

In Fig. Ia consider a point source of strength Q nuetrons/sec at a point on the x-axis ℓ cm from the origin. The number of neutrons incident on the elemental surface ds is

$$\frac{Q}{4\pi R^2} r^2 \sin\theta \, d\theta \, d\phi \, \cos\psi \ . \tag{I-1}$$

All quantities are defined in the diagram (Fig. Ia). The probability for fission in this surface is given by

$$\frac{(\rho t)(6.023)(10^{23})}{238} \ \bar\sigma_f \ \frac{1}{\cos\psi} , \tag{I-2}$$

where ρ is the density and t the thickness of U^{238} on the hemisphere. $\bar\sigma_f$ is the average fission cross section of U^{238} for neutrons from the source. The number of fissions in ds, dN_{28}, is from Eqs. (I-1) and (I-2),

$$dN_{28} = \left[\frac{Q}{4\pi R^2} r^2 \sin\theta \, d\theta \, d\phi \, \cos\psi\right]\left[\frac{\rho t(6.023)(10^{23})}{238} \ \bar\sigma_f \ \frac{1}{\cos\psi}\right]$$

or

$$N_{28} = \frac{(6.023)(10^{23})}{(4\pi)\,(238)} \ \bar\sigma_f \ \rho t \, Q \int_{\theta=0}^{\theta=\pi} \int_{\phi=\pi/2}^{\phi=\pi/2} \frac{r^2 \sin\theta \, d\phi \, d\theta}{R^2} . \tag{I-3}$$

Substitution of $R^2 = \ell^2 + r^2 - 2\ell r \cos\theta$ \hfill (I-4)

and Eq. (I-4) into Eq. (I-3) gives:

$$N_{28} = \frac{(6.023)(10^{23})}{(4\pi)\,(238)} \ \bar\sigma_f \rho t \, Q \int_{\theta=0}^{\theta=\pi} \int_{\phi=\pi/2}^{\phi=\pi/2} \frac{r^2 \sin\theta \, d\phi \, d\theta}{\ell^2 + r^2 - 2\ell r \cos\theta} . \tag{I-5}$$

Carrying out the integration, we obtain:

$$N_{28} = \frac{(6.023)(10^{23})}{(4\pi)\,(238)} \ \pi\bar\sigma_{f,} \rho t \, Q \int_{\theta=0}^{\theta=\pi} \int_{\phi=-\pi/2}^{\phi=\pi/2} \frac{r^2 \sin\theta \, d\theta}{\ell^2 + r^2 - 2\ell r \cos\theta}$$
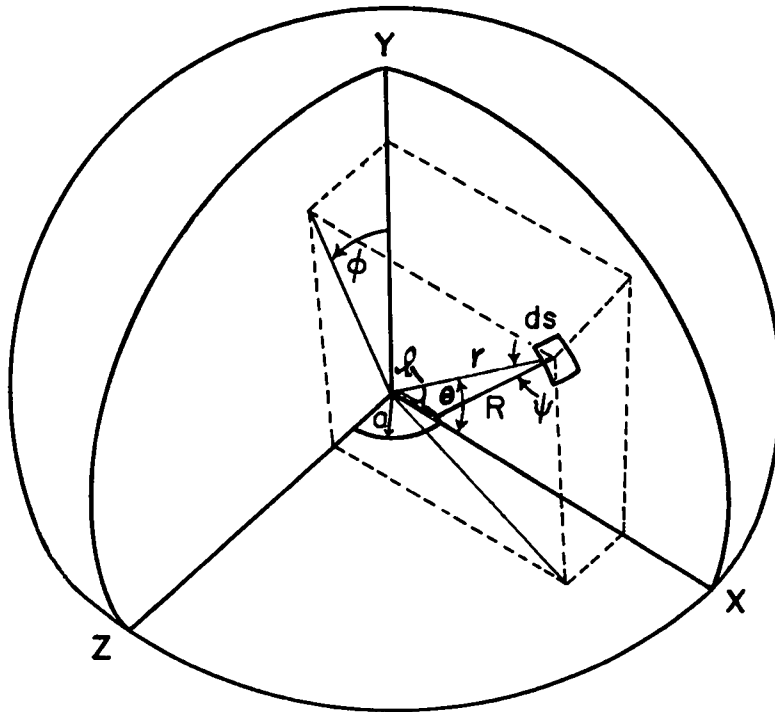
- 18 -
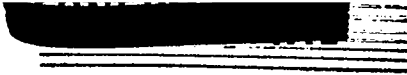
Fig. Ia Hemispherical geometry for cross section measurement.

$$= \frac{(6.023)\,(10^{23})}{(4)\,(238)}\,\frac{\bar{\sigma}_f\,\rho t\,Qr^2}{2\ell r}\ln\,(\ell^2 + r^2 - 2\ell r\,\cos\theta)\ \Big|_{\theta=0}^{\pi}$$

Therefore,

$$N_{28} = \frac{(6.023)\,(10^{23})}{(4)\,(238)}Q\bar{\sigma}_f\rho t\,\frac{r}{\ell}\,\ln\,\frac{r+\ell}{r-\ell}\,, \tag{I-6}$$

which is the equation that applies for a point source of neutrons.

Now, in practice, the source is not a point but a disc. Therefore, let us take Q as the number of neutrons per second emanating from an elemental ring da of the disc. Thus:

$$Q = q\,da = 2\pi q\ell\,d\ell\,, \tag{I-7}$$

where q is the number of neutrons per square centimeter per second emitted from the disc. Substituting Eq. (I-7) in Eq. (I-6) and integrating over the entire disc source, we obtain for a disc source:

$$N_{28} = \int_{\ell=0}^{\ell=a} 2\pi\,\frac{(6.023)\,(10^{23})}{(4)\,(238)}\,q\bar{\sigma}_f\rho t\frac{r}{\ell}\,\ell\,\ln\frac{r+\ell}{r-\ell}\,d\ell$$

$$= \frac{(2\pi)\,(6.023)\,(10^{23})}{(4)\,(238)}\,q\bar{\sigma}_f\rho t\,r\int_{\ell=0}^{\ell=a}\big[\ln(r+\ell) - \ln(r-\ell)\big]\,d\ell$$

$$= \frac{\pi\,(6.023(\,(10^{23})}{(2)\,(238)}\,q\bar{\sigma}_f\rho t\,r\,\big[\,(r+\ell)\,\ln\,(r+\ell) - (r+\ell) +$$

$$(r-\ell)\,\ln\,(r-\ell) - (r-\ell)\big]\ \Big|_{\ell=0}^{\ell=a}$$

$$= \frac{\pi\,(6.023)\,(10^{23})}{(2)\,(238)}\,q\bar{\sigma}_f\rho t\,r\left[r\,\ln\!\left(\frac{r^2 - a^2}{r^2}\right) + a\,\ln\,\frac{r+a}{r-a}\right]\,. \tag{I-8}$$

The mass of U^{238} on the hemisphere can be written

$$M_{28} = 2\pi r^2\rho t, \tag{I-9}$$

or

$$\rho tr = \frac{M_{28}}{2\pi r}$$

Substituting Eq. (I-9) into Eq. (I-8), we have

$$N_{28} = \frac{(6.023)(10^{23})}{(4)(238)} q\, M_{28}\, \bar{\sigma}_f \left[\ln\left(\frac{r^2 - a^2}{r^2}\right) + \frac{a}{r} \ln\left(\frac{r+a}{r-a}\right) \right]. \qquad (I-10)$$

If the source is U^{235}, the number of neutrons emitted per square centimeter of the U^{235} can be written

$$q = \frac{N_{25}\nu}{\pi a^2} , \qquad (I-11)$$

where N_{25} is the number of fissions in the U^{235} source and ν is the average number of neutrons emitted per fission of U^{235}. Substituting Eq. (I-11) into Eq. (I-10), we obtain

$$N_{28} = \frac{(6.023)(10^{23})}{(4\pi)(238)} M_{28}\, N_{25}\, \nu\, \bar{\sigma}_f \frac{1}{a^2} \left[\ln\left(\frac{r^2 - a^2}{r^2}\right) + \frac{a}{r} \ln\left(\frac{r+a}{r-a}\right) \right], \qquad (I-12)$$

which is the equation from which we determine $\bar{\sigma}_f$.

APPENDIX II

NON-UNIFORMITY CONSIDERATIONS

The geometric calculations of Appendix I were carried out on the basis of uniform thickness t of U^{238}. To determine the effect of non-uniformity of the U^{238} on the hemisphere, we consider the extreme cases: (1) concentration of material at pole and (2) concentration of material in a band at the equator.

Case 1. Concentration of Material at Pole.

Consider Fig. Ia with the element of area Δs at the pole so that $\theta \cong 0$. From a point source at ℓ, the flux of neutrons on Δs at the pole would be given by

$$\frac{Q \cos \psi}{4 \pi (\ell^2 + r^2)} . \tag{II-1}$$

The same symbols are used here as were used in Appendix I where ϕ and θ are the angle coordinates. The probability for fission of the U^{238} by these neutrons is given by

$$\frac{(6.023)(10^{23})}{(238)} \frac{\rho t \bar{\sigma}_f}{\cos \psi} . \tag{II-2}$$

Therefore, the total number of fissions per second in the U^{238} at the pole that are induced by the point source of neutrons is

$$N_{28p} = \frac{Q}{4\pi(\ell^2 + r^2)} \rho t \bar{\sigma}_f \frac{(6.023)(10^{23})}{238} . \tag{II-3}$$

Re-defining Q so that $dQ = q \ell d\ell d\alpha$, where q is the number of neutrons per square centimeter per second from disc, and integrating over the disc, we find

$$N_{28p} = \frac{(6.023)(10^{23})}{(4\pi)(238)} \frac{N_{25}\nu}{a^2} M_{28} \bar{\sigma}_f \ln \left(\frac{a^2 + r^2}{r^2} \right) \tag{II-4}$$

Comparing Eq. (II-4) with Eq. (I-12), we find

$$\frac{N_{28p}}{N_{28}} = \frac{\ln \left(\frac{r^2 + a^2}{r^2} \right)}{\left[\ln \left(\frac{r^2 - a^2}{r^2} \right) + \frac{a}{r} \ln \left(\frac{r + a}{r - a} \right) \right]} . \tag{II-5}$$

- 22 -
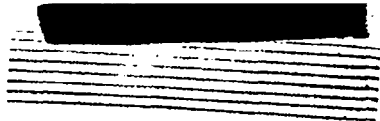
Letting $\frac{a}{r} = x$, Eq. (II-5) can be written

$$\frac{N_{28p}}{N_{28}} = \frac{\ln(1 + x^2)}{\ln(1 - x^2) + x\ln\left(\frac{1 + x}{1 - x}\right)}.$$

(II-6)

Expanding the numerator and denominator and dividing, we obtain

$$\frac{N_{28p}}{N_{28}} = 1 - \frac{2}{3}x^2 + \frac{17}{45}x^4 ---------- .$$

(II-7)

To conform with the < 1 percent accuracy of the experiment, we shall ask that even if all the U^{238} were at the pole the number of U^{238} fissions shall not exceed that for a uniform U^{238} deposit by more than about 1 percent. That is,

$$0.99 \leqslant \frac{N_{28p}}{N_{28}} \leqslant 1.01 .$$

Solving for x, we find

$$x \leqslant 0.12.$$

Case 2. Concentration of Material at the Equator.

Consider the U^{238} concentrated in a band at the equator of the hemisphere. Thus, in Fig. Ia, $\theta \cong \pi/2$. Since the mean square distance of any point on the source disc from the hemisphere equator as obtained from $\int_0^{2\pi} R^2 d\alpha / \int_0^{2\pi} d\alpha$ is $(r^2 + \ell^2)$, which also is the distance from the pole of any point on the disc, the problem for this case is just the same as that for Case 1.

We conclude, therefore, that if the ratio of the disc radius to hemisphere radius satisfies the relation

$$\frac{a}{r} \leqslant 0.12 ,$$

then the relation

$$0.99 \leqslant \frac{N_{28}'}{N_{28}} \leqslant 1.01$$

- 23 -

is also satisfied, where N_{28} is the number of fissions observed when the U^{238} is distributed in the extremely non-uniform ways described above, and where N_{28} is the number of fissions observed when the U^{238} is uniformly distributed over the hemisphere.

Since the value of a/r for the experimental apparatus is 0.15 and since the U^{238} deposit appeared to be uniform over the hemisphere, it is felt that there is no appreciable error from this possibility.

APPENDIX III

U^{238} FISSIONS INDUCED BY NEUTRONS SCATTERED FROM REACTOR FACE

A small fraction, which is to be computed, of the U^{238} fissions are induced by fission neutrons scattered from the reactor face at energies above the fission threshold. Although some fissions are similarly induced by floor scattering, this number can be shown to be negligibly small.

The computation of the effect of the reactor face involves the use of the albido, which is an expression for the fractional return of neutrons entering a reflecting and absorbing medium. For an infinitely deep material the albido is

$$A = \frac{1 - 2\sqrt{\dfrac{\sigma_a}{3\sigma_t}}}{1 + 2\sqrt{\dfrac{\sigma_a}{3\sigma_t}}},$$

where σ_a and σ_t are the absorption and the transport cross section, respectively. For fission spectrum neutrons in lead, the first material of considerable depth in the reactor, the total cross section is ~ 6 barns, as given in AECU-2040. Similarly, the cross section for inelastic collisions lowering the neutron energy below the U^{238} fission threshold (which here is effectively the absorption cross section) is found to be 0.74 barn from the measurements by Jurney.*

On this basis, we use $\sigma_a = 0.74$ barn and $\sigma_t = (6 - 0.74)(1 - \overline{\cos\theta})$, where $\overline{\cos\theta} = 2/(3M)$. Since for lead $M = 207$, we have $\sigma_t = 5.2$ barns. Substitution in the albido expression yields $A = 0.39$.

Having the fractional return of neutrons effective for fission, we now find through inverse square distance considerations the scattered flux on the hemisphere. Involved are the distance from the fission source to the reactor and some effective distance between the U^{238} hemisphere surfaces and the reactor. With the source being 30 cm from the reactor in the experiment, we take, for simplicity, $d = 32$ cm for the effective distance applying to both. The number of neutrons incident upon an elementary ring on the reactor face at distance r and angle θ (θ is the angle between d and r) is

$$\frac{Q \, 2\pi r^2 \sin\theta \, d\theta}{4\pi r^2}.$$

---

*E. T. Jurney, LA-1339 (December 1951).

However, as seen above, of these neutrons only 0.39 will be re-emitted with adequate energy for fission. These will be emitted with isotropic distribution into 2π solid angle. Thus the effective flux of neutrons from this scattering element is

$$\frac{Q\ 2\pi r^2\ \sin\theta\ d\theta}{4\pi r^2}\ \ \frac{(0.39)}{2\pi r^2} \ .$$

Substitution of $d = r\cos\theta$ yields

$$\frac{(0.39)\ Q}{4\pi d^2}\ \ \cos^2\theta\ \sin\theta\ d\theta$$

The total scattered flux is found by integrating over all such scattering elements. The minimum angle of integration as defined by the exit hole for thermal neutrons is $\sim \tan^{-1} 0.2$. On the other hand, the maximum angle is essentially $\pi/2$. The scattered flux in the $d = 32$ cm vicinity of the source and hemisphere is then

$$(nv)_s \cong \int_{\theta=\tan^{-1}0.2}^{\pi/2} \frac{0.39\ Q}{4\pi d^2}\ \cos^2\theta\ \sin\theta\ d\theta$$

$$\cong \frac{0.39\ Q}{(3)\ (4)\pi d^2}\ \cos^3\theta\ \Big|_{\tan^{-1}0.2}^{\pi/2}$$

$$\cong \frac{1.19(10^{-4})Q}{4\pi}\ \ n/cm^2/sec.$$

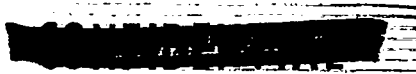The primary flux of fission neutrons on the 7.6-cm radius hemisphere is

$$(nv)_p \cong \frac{Q}{4\pi(7.6)^2}\ = \frac{1.73(10^{-2})Q}{4\pi}\ \ n/cm^2/sec.$$

Then the relative fluxes and, consequently, the relative number of fissions is

$$\frac{(nv)_s}{(nv)_p} \cong \frac{1.19(10^{-4})}{1.73(10^{-2})}\ = \ 0.69(10^{-2}).$$

A correction for this quantity is included in the cross sections in Table 1.

APPENDIX IV

CORRECTION FOR FISSIONS CAUSED BY NEUTRONS SCATTERED
FROM HEMISPHERES

Consider first the neutrons scattered from the aluminum hemisphere on which the $U_3^{238}O_8$ is painted. In Fig. IVa, $(r_2 - r_1)$ is the $U_3^{238}O_8$ thickness, t is the thickness of U_3O_8 "seen" by a neutron scattered at point P in the Al.

To simplify the calculations, we consider now an entire sphere so that, by symmetry, all scattering from points on the spherical radius $r_1 - \delta$ can be regarded as occurring at P.

In the triangle (r_1, r_2, t) the law of cosines gives

$$r_2^2 = r_1^2 + t^2 - 2r_1 t \cos(\pi - \alpha), \tag{IV-1}$$

or

$$t = - r_1 \cos \alpha + \sqrt{r_1^2 \cos^2 \alpha + r_2^2 - r_1^2} . \tag{IV-2}$$

The probability for fission by this scattered neutron is

$$\frac{(6.023)(10^{23}) \rho_u t \bar{\sigma}_f}{238} \tag{IV-3}$$

where ρ_u is the U^{238} density in $U_3^{238}O_8$ and t is given by Eq. (IV-2).

Consider now a sphere of radius R and center at P. The number of neutrons per square centimeter incident on this sphere is $\frac{Q}{4\pi R^2}$, where Q is the total number of neutrons scattered at P. Therefore, the total number of fissions induced by these neutrons and occurring per unit area of this sphere is, by Eq. (IV-3),

$$\frac{(6.023)(10^{23}) \rho_u \bar{\sigma}_f Q}{(238)(4\pi R^2)} \left(-r_1 \cos\alpha + \sqrt{r_1^2 \cos^2 \alpha + r_2^2 - r_1^2} \right) . \tag{IV-4}$$

The area of a circular element of the sphere about P is $2\pi R^2 \sin\beta \, d\beta$; for all points of this element the value of t is constant. Therefore, the number of fissions which occur in a circular element (the center of which is on the x axis) of a sphere with a diameter of R, center at P, is

$$dN = \frac{(6.023)(10^{23}) Q \bar{\sigma}_f \rho_u}{(238)(4\pi R^2)} \left(-r_1 \cos \alpha + \sqrt{r_1^2 \cos^2 \alpha + r_2^2 - r_1^2} \right) 2\pi R^2 \sin\beta \, d\beta. \tag{IV-5}$$
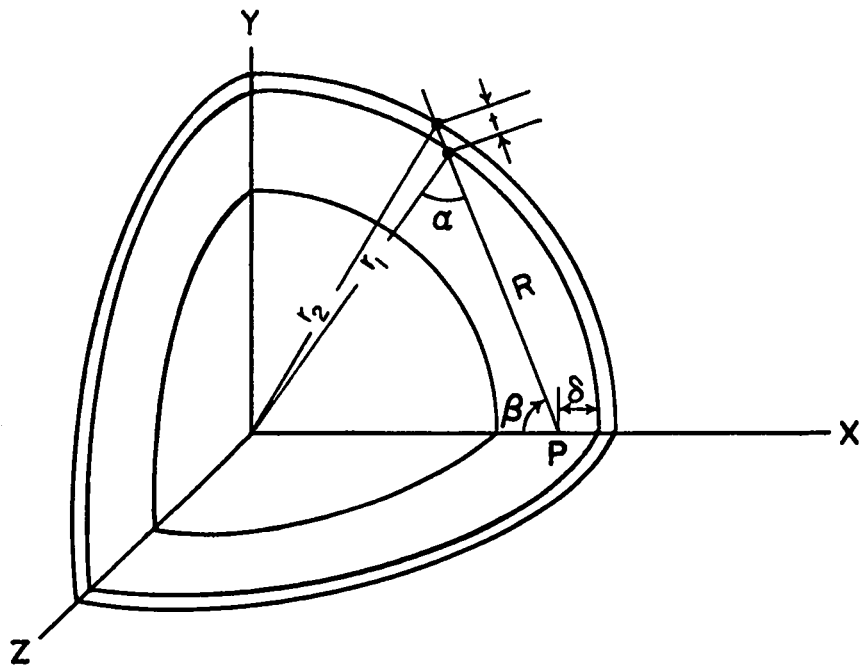
Fig. IVa Geometry of neutron scattering from uranium backing hemisphere.

Thus, the total number of fissions caused by neutrons scattered at P is given by

$$N = \int_{\beta=0}^{\beta=\pi} \frac{(6.023)(10^{23}) Q \bar{\sigma}_f \rho_u}{(238)(2)} \left(-r_1 \cos\alpha + \sqrt{r_1^2 \cos^2\alpha + r_2^2 - r_1^2}\right) \sin\beta \, d\beta, \qquad \text{(IV-6)}$$

where the limits of integration include the 4π solid angle about P.

To integrate this expression, we must relate α and β. To do this we use the law of sines and other trigonometric relations as follows:

In triangle $(r_1, R, r_1 - \delta)$,

$$\frac{\sin\alpha}{\sin\beta} = \frac{r_1 - \delta}{r_1}. \qquad \text{(IV-7)}$$

Thus,

$$\sin\beta = \frac{r_1}{r_1 - \delta} \sin\alpha, \qquad \text{(IV-7')}$$

and

$$\cos\beta = \frac{\sqrt{r_1^2 \cos^2\alpha - 2r_1 \delta + \delta^2}}{r_1 - \delta}. \qquad \text{(IV-8)}$$

Also, from Eq. (IV-7'),

$$\cos\beta \, d\beta = \frac{r_1 \cos\alpha}{r_1 - \delta} \, d\alpha,$$

and

$$d\beta = \frac{r_1}{r_1 - \delta} \frac{\cos\alpha}{\cos\beta} \, d\alpha,$$

or

$$d\beta = \frac{r_1 \cos\alpha}{\sqrt{r_1^2 \cos^2\alpha - 2r_1 \delta + \delta^2}} \, d\alpha. \qquad \text{(IV-9)}$$

Combining Eq. (IV-7') and Eq. (IV-9), we get

$$\sin\beta \; d\beta = \frac{r_1}{r_1 - \delta} \; \frac{\sin\alpha \; \cos\alpha}{\sqrt{\cos^2\alpha - \dfrac{2\delta}{r_1} + \dfrac{\delta^2}{r_1^2}}} d\alpha. \qquad (IV-10)$$

Substituting Eq. (IV-10) into Eq. (IV-6), we find

$$N = \int_{\beta=0}^{\beta=\pi} \frac{(6.023)\,(10^{23})}{(2)\,(238)} \; \frac{r_1 Q\bar\sigma_f \rho_u}{r_1 - \delta} \left(-r_1\cos\alpha + \sqrt{r_1^2 \cos^2\alpha + r_2^2 - r_1^2} \; \frac{\sin\alpha \; \cos\alpha}{\sqrt{\cos^2\alpha - \dfrac{2\delta}{r_1} + \dfrac{\delta^2}{r_1}}} \right) d\alpha.$$

If we define

$$K \equiv \frac{(6.023)\,(10^{23})}{(2)\,(238)} \; \frac{r_1 Q\,\bar\sigma_f \rho_u}{1 - \dfrac{\delta}{r_1}}, \qquad (IV-11)$$

then

$$N = K \int_{\beta=0}^{\beta=\pi} \left[\frac{\cos^2\alpha + \dfrac{r_2^2 - r_1^2}{r_1^2}}{\cos^2\alpha - \dfrac{2\delta}{r_1} + \dfrac{\delta^2}{r_1^2}} \right]^{1/2} \sin\alpha \; \cos\alpha \; d\alpha \qquad (IV-12)$$

$$-K \int_{\beta=0}^{\beta=\pi} \frac{\sin\alpha \; \cos^2\alpha \; d\alpha}{\sqrt{\cos^2\alpha - \dfrac{2\delta}{r_1} + \dfrac{\delta^2}{r_1^2}}}$$

also, if we define

$$\Delta^2 \equiv \frac{r_2^2 - r_1^2}{r_1^2} \qquad (IV-13)$$

and substitute Eq. (IV-13) into Eq. (IV-12), then

$$N = K \int_{\beta=0}^{\beta=\pi} \left[\frac{\cos^2\alpha + \Delta^2}{\cos^2\alpha - \dfrac{2\delta}{r_1} + \dfrac{\delta^2}{r_1}} \right]^{1/2} \sin\alpha \; \cos\alpha \; d\alpha - K \int_{\beta=0}^{\beta=\pi} \frac{\sin\alpha \; \cos^2\alpha \; d\alpha}{\sqrt{\cos^2\alpha - \dfrac{2\delta}{r_1} + \dfrac{\delta^2}{r_1^2}}} \qquad (IV-14)$$

- 30 -

This equation is the general expression for the number of fissions induced by neutrons scattered at the depth δ .

Since, for the mean scattering depth at $\delta \cong 0.01$ in., $\cos^2 \alpha$ never approaches zero and, indeed, is very large compared to Δ^2, we can expand the numerator of the first integral in Eq. (IV-14), thus

$$(\cos^2\alpha + \Delta^2)^{1/2} = \cos\alpha + \frac{\Delta^2}{2\cos\alpha} - \frac{\Delta^4}{8\cos^3\alpha} + \frac{\Delta^6}{16\cos^5\alpha} \text{----------,} \quad \text{(IV-15a)}$$

which, when substituted into Eq. (IV-14), gives

$$N = K \left\{ \frac{\Delta^2}{2} \int_{\beta=0}^{\beta=\pi} \frac{\sin\alpha \, d\alpha}{\left(\cos^2\alpha - \frac{2\delta}{r_1} + \frac{\delta^2}{r_1^2}\right)^{1/2}} - \frac{\Delta^4}{8} \int_{\beta=0}^{\beta=\pi} \frac{\sin\alpha \, d\alpha}{\cos^2\alpha\left(\cos^2\alpha - \frac{2\delta}{r_1} + \frac{\delta^2}{r_1^2}\right)^{1/2}} \right.$$

$$\left. + \frac{\Delta^6}{16} \int_{\beta=0}^{\beta=\pi} \frac{\sin\alpha \, d\alpha}{\cos^4\alpha\left(\cos^2\alpha - \frac{2\delta}{r_1} + \frac{\delta^2}{r_1^2}\right)^{1/2}} + \text{--------------} \right\}. \quad \text{(IV-15)}$$

Now we determine the limits of integration for α. Obviously, $\alpha = 0$ both for $\beta = 0$ and $\beta = \pi$, so we use the equations preceding Eq. (IV-9), which give

$$\frac{d\alpha}{d\beta} = \frac{r_1 - \delta}{r_1} \frac{\cos\beta}{\cos\alpha} \quad .$$

Setting this equal to zero, we find that $\beta = \frac{\pi}{2}$ and $\alpha = \sin^{-1}\frac{r_1-\delta}{r_1}$ for maximum α. Next we divide each of the integrals in Eq. (IV-15) into two integrals, one for the limits zero and $\sin^{-1}\frac{r_1-\delta}{r_1}$, the other for the limits $\sin^{-1}\frac{r_1-\delta}{r_1}$ and π. The first term of Eq. (IV-15) is

$$\frac{K\Delta^2}{2} \int_{\alpha=0}^{\alpha=\sin^{-1}\frac{r_1-\delta}{r_1}} \frac{\sin\alpha \, d\alpha}{\left(\cos^2\alpha - \frac{2\delta}{r_1} + \frac{\delta^2}{r_1^2}\right)^{1/2}} + \frac{K\Delta^2}{2} \int_{\alpha=\sin^{-1}\frac{r_1-\delta}{r_1}}^{\alpha=0} \frac{\sin\alpha(-d\alpha)}{\left(\cos^2\alpha - \frac{2\delta}{r_1} + \frac{\delta^2}{r_1^2}\right)^{1/2}},$$

which, when integrated is

$$\frac{K\Delta^2}{2} \ln\left(\frac{2r_1-\delta}{\delta}\right) . \quad \text{(IV-16)}$$

- 31 -

The second term of Eq. (IV-15), similarly evaluated, is

$$\frac{K\Delta^4}{4} \ \frac{r_1\left(r_1 - \delta\right)}{\delta\left(2r_1 - \delta\right)} \ . \tag{IV-17}$$

Substituting Eqs. (IV-16) and (IV-17) into (IV-15), we get

$$N = \frac{K\Delta^2}{2} \ \ln\left(\frac{2r_1 - \delta}{\delta}\right) + \frac{K\Delta^4 \, r_1 \left(r_1 - \delta\right)}{4\,\delta\left(2r_1 - \delta\right)}. \tag{IV-18}$$

It can be shown by the following analysis that the second term in Eq. (IV-18) is very small compared to the first term. The ratio of the two terms is

$$\frac{\Delta^2 \, r_1 \left(r_1 - \delta\right)}{2\,\delta \left(2r_1 - \delta\right) \ln\left(\frac{2r_1 - \delta}{\delta}\right)} \ .$$

In this experiment, $r_1 \cong 3$ in., $\Delta^2 \cong 2.5(10^{-6})$, and we consider the mean scattering distance $\delta \cong 0.010$ in. For these values, the above ratio is much less than unity. Therefore, Eq. (IV-18) reduces to

$$N \cong \frac{K\Delta^2}{2} \ \ln\left(\frac{2r_1 - \delta}{\delta}\right). \tag{IV-19}$$

Equation (IV-19) gives N, assuming that all scattering takes place on a sphere of radius $(r_1 - \delta)$. It can be shown that when distributed scattering centers are taken into account, the value for N is not appreciably different from that given by Eq. (IV-19). Also, isotropic scattering of fast neutrons from the aluminum hemisphere has been assumed in deriving Eq. (IV-19); however, if the angular distribution of fast neutrons scattered from aluminum as measured by Jurney (LA-1339) is used in these calculations rather than a simple isotropic scattering, the result for the number of fissions N in the U^{238} coating from scattered neutrons is calculated to be ~ 7 percent greater than that given by Eq. (IV-19).

It remains now to determine the value of N for the actual hemispherical geometry of this experiment (Eq. (IV-19) is valid for spherical geometry). This is done in the following way: (a) N is calculated, assuming that all actual scattering points on the hemisphere "see" the actual hemisphere in the same geometry as the polar scattering point of the calculations "sees" its hemisphere, (b) N is calculated, assuming that all actual scattering points "see" the actual hemisphere just as an equatorial scattering point of the calculations "sees" a hemisphere, (c) a compromise between the two extreme values thus obtained is reached by the reasonable

considerations described below to give the value of N we use. The result for calculation (a) is obtained by subtracting from the total-sphere value of N calculated from Eq. (IV-19) the value of N obtained by integrating Eq. (IV-15) from $\beta = 0$ to $\beta = \tan^{-1} \frac{r_1}{r_1 - \delta}$. The result for calculation (b) is obtained simply by dividing the total-sphere value of N from Eq. (IV-19) by two.

It is readily seen that the scattered neutrons which "see" the greatest thickness of U^{238} are those with β roughly $\pi/2$. Because of this, a very large fraction of the fissions induced by scattered neutrons are in a very small area of the U^{238} deposit surrounding the scattering point. A consideration, such as (a) above, which completely takes into account this sensitive area surrounding the scattering points is a more accurate representation of the actual situation of scattering points over the entire hemisphere than is a consideration, such as (b) above, which takes into account only half the area surrounding a point. Indeed, it appears that (b) would be approximately correct only for a small band of aluminum around the equator that is within a distance of about (10^{-1}) or (10^{-2}) centimeters from the edge of the U^{238} deposit. Therefore, the result of calculation (a) is weighted with respect to the result of calculation (b) in the somewhat arbitrary ratio of 20:1.

The result of these calculations is

$$N \cong (0.023)N_p \qquad \text{(IV-20)}$$

where N_p is the number of U^{238} fissions caused by primary (unscattered) fast neutrons.

To calculate the number of U^{238} fissions caused by fast neutrons scattered from the hemispherical copper case, consider Fig. IVb. The integral equation for N can be set up in a way similar to that described at the beginning of this Appendix for the case of the aluminum backing hemisphere. The resulting equation, which corresponds to Eq. (IV-14) in the previous case, is

$$N = K' \left\{ \int_{\alpha_2=0}^{\pi/2} \frac{\cos^2\alpha_2 \, \sin\alpha_2 \, d\alpha_2}{A_2^{1/2}} - \int_{\alpha_2=0}^{\pi/2} \left[\frac{\cos^2\alpha_2 - (\Delta')^2}{A_2} \right] \sin\alpha_2 \, \cos\alpha_2 \, d\alpha_2 \right. \qquad \text{(IV-21)}$$

$$\left. + \int_{\alpha_1=\pi/2}^{\pi} \frac{\cos^2\alpha_1 \, \sin\alpha_1 \, d\alpha_1}{A_1^{1/2}} - \int_{\alpha_1=\pi/2}^{\pi} \left[\frac{\cos^2\alpha_1 - (\Delta')^2}{A_1} \right]^{1/2} \sin\alpha_1 \, \cos\alpha_1 \, d\alpha_1 \right\},$$
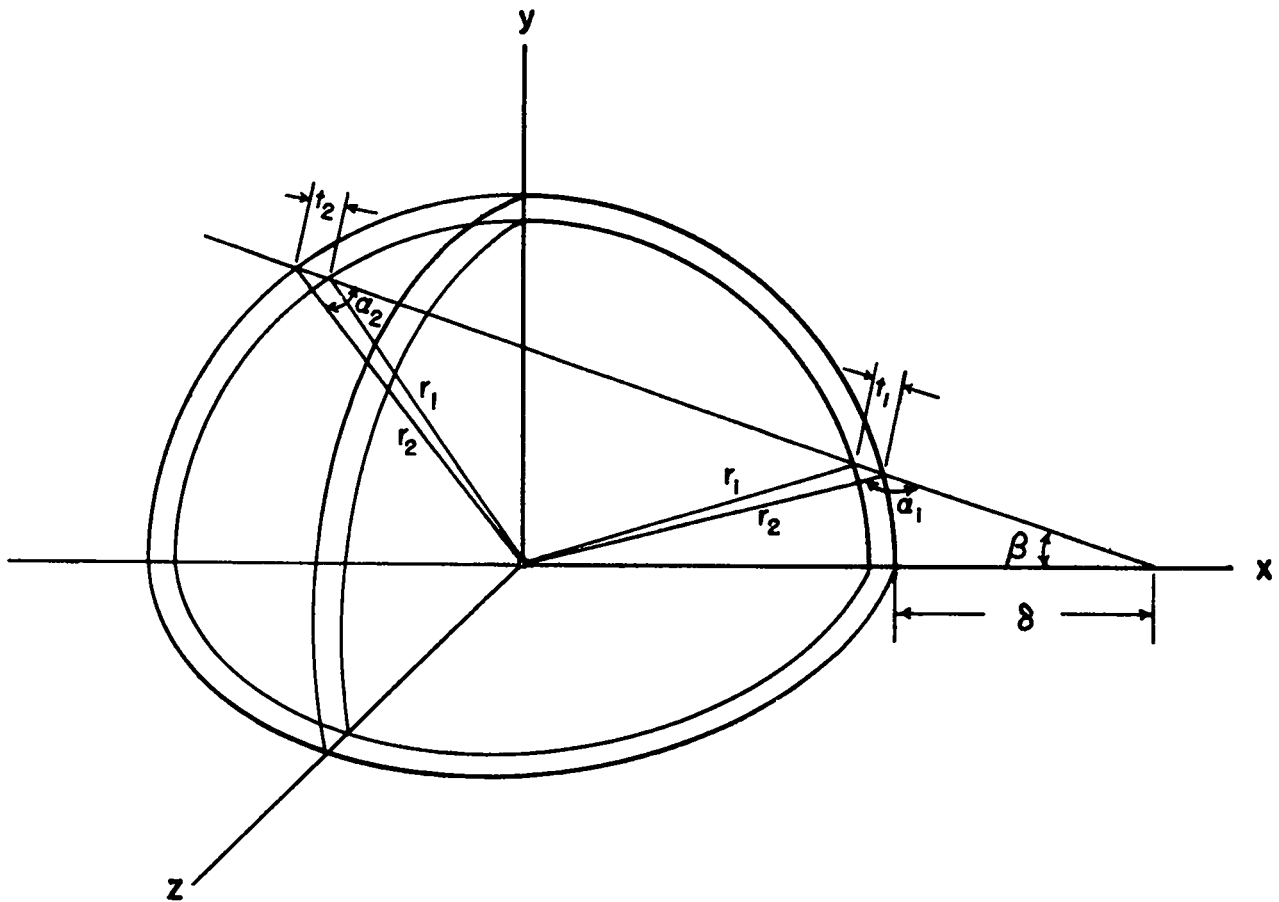
Fig IVb Geometry of neutron scattering from outer hemispheres.

where

$$A_1 = \cos^2\alpha_1 + \frac{2\delta}{r_2} + \frac{\delta^2}{r_2^2}$$

$$A_2 = \cos^2\alpha_2 + \frac{2\delta}{r_2} + \frac{\delta^2}{r_2}$$

$$K' = \frac{(6.023)(10^{23}) Q \sigma_f \rho_u}{(2)(238)} \quad \frac{r_2^2}{r_2 + \delta} \quad . \tag{IV-22}$$

$$(\Delta')^2 = \frac{r_2^2 - r_1^2}{r_2^2} \tag{IV-23}$$

In Eq. (IV-21), the third and fourth integrals involve the passage of neutrons into the spherical U^{238} shell under consideration. The first and second integrals involve the exit of neutrons from this shell. Expanding, and carrying out the integrations as before, we obtain

$$N = \frac{K'(\Delta')^2}{2} \ln \frac{2r_2 + \delta}{8} + \frac{K'(\Delta')^4}{4} \left[\frac{1 - \frac{2\delta}{r_2} - \frac{\delta^2}{r_2^2}}{\left(\frac{2\delta}{r_2} + \frac{\delta^2}{r_2^2}\right)\left(1 + \frac{\delta}{r_2}\right)} \right] \quad . \tag{IV-24}$$

Since again the second term is small compared to the first term, we have, for spherical geometry, the result

$$N \cong \frac{K'(\Delta')^2}{2} \quad \ln \left(\frac{2r_2 + \delta}{\delta}\right). \tag{IV-25}$$

Now to determine K' (Eq. (IV-22)), Q, the source strength of the scattered neutrons, must be known and to find this we use the angular distribution of scattered neutrons from copper as measured by Jurney (LA-1339). Since only back-scattered neutrons are effective only the back-scattering cross section is used.

The value of N for hemispherical geometry is again obtained first for two simplified cases: (a) assuming that all scattering takes place at the pole, (b) assuming that all scattering takes place at the equator. Results for case (a) are obtained by substituting $\alpha_2 = \tan^{-1} \frac{r_2 + \delta}{r_2}$ as the lower limits of the first and second integrals in Eq. (IV-25). This removes the contribution of the exit neutrons through the lower hemisphere. Results for case (b) are obtained, as before, by dividing the total-sphere value of Eq. (IV-25) by two. The method by which the

average is to be taken is not as clear here as in the case of the aluminum backing hemisphere. However, from the dimensions of the two hemispheres and from their relation in space, somewhat arbitrary assignments of weight two to the polar value and unity weight to the equatorial value seem reasonable.

The value thus obtained for N, the number of U^{238} fissions caused by fast neutrons scattered from the copper case, is given by

$$N = (0.0051)N_p \qquad\qquad\qquad (IV\text{-}26)$$

Analysis similar to the above can be made to determine the number of U^{238} fissions caused by fast neutrons scattered from the aluminum collecting hemisphere and the cadmium shield. The results of these calculations are, respectively, $N = (0.002)N_p$ and $N = (0.019)N_p$.

APPENDIX V
ATTENUATION AND SCATTERING OF THERMAL NEUTRONS BETWEEN
MONITOR FOIL AND DISC SOURCE

In this Appendix we shall be concerned with the fact that some of the fissions induced in the U^{235} disc source and monitor foil are caused by thermal neutrons which have been scattered from the dural plate between the disc source and monitor foil.

We simplify the calculation of this effect by assuming that all scattering takes place in a single surface midway between the faces of the dural plate (see Fig. Va).

The number of neutrons scattered from dA into da is given by

$$\frac{q \cos \psi \; dA \; da}{4\pi R^2} \tag{V-1}$$

where

$$q = (nv)_{th} \left(\frac{\rho t N \sigma_s}{A} \right)_{Al}. \tag{V-2}$$

In Eq. (V-2), $(nv)_{th}$ is the thermal neutron flux from the reactor. The quantities ρ, t, A, and σ_s are the density, thickness, mass number, and scattering cross section, respectively. Avogadro's number is expressed as N.

The number of fissions induced in da from these scattered neutrons is given by

$$\left(\frac{\rho t N \sigma_f}{A} \right)_U \left(\frac{q \; dA \; da}{4\pi R^2} \right), \tag{V-3}$$

where the subscript U refers to the U^{235} disc source. Now the number of fissions in area a from the neutrons scattered in dA is

$$dN_U = \frac{q \; dA}{4\pi} \left(\frac{\rho t N \sigma_f}{A} \right)_U \int_{\theta=0}^{2\pi} \int_{r=0}^{r_o} \frac{r \; dr \; d\phi}{b^2 + \ell^2 + r^2 - 2r\ell \cos(\theta - \phi)}, \tag{V-4}$$

and the total number of fissions in area A induced by neutrons scattered in the entire area A is

$$N_U = \frac{q}{4\pi} \left(\frac{\rho t N \sigma_f}{A} \right)_U \int_{\theta=0}^{2\pi} \int_{\ell=0}^{\ell_o} \ell \; d\ell \, d\theta \int_{\phi=0}^{2\pi} \int_{r=0}^{r_o} \frac{r \; dr \; d\phi}{b^2 + \ell^2 + r^2 - 2r\ell \cos(\theta - \phi)}, \tag{V-5}$$
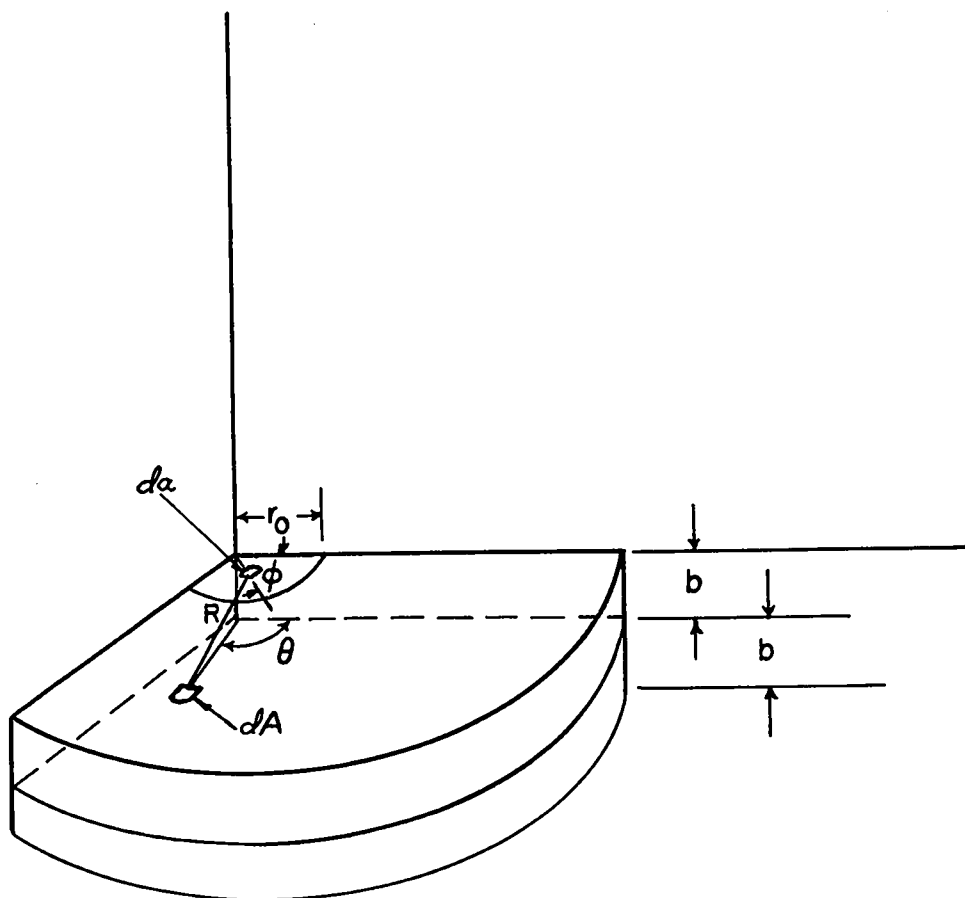
Fig. Va Geometry of neutron scattering in the U^{235} source plate.

where we have used the relations:

$$R^2 = b^2 + \ell^2 + r^2 - 2r\ell \cos(\theta - \phi) \tag{V-6}$$

$$da = r \, dr \, d\phi$$

$$dA = \ell \, d\ell \, d\phi.$$

The total number of fissions in the disc source of area a caused by unscattered thermal neutrons incident on it after passage through the aluminum is given by

$$N'_U = (nv)_{th} \, a\left(\frac{\rho t N \sigma_f}{A}\right)_U \left[1 - \left(\frac{\rho t N \sigma_t}{A}\right)_{Al}\right] \quad , \tag{V-7}$$

so that the ratio of the number of fissions from scattered neutrons to the number of fissions from direct neutrons can, using Eq. (V-2), be written

$$\frac{N_U}{N'_U} = \frac{\left(\frac{\rho t N \sigma_s}{A}\right)_{Al} I}{4\pi a \left[1 - \left(\frac{\rho t N \sigma_t}{A}\right)_{Al}\right]}, \tag{V-8}$$

where

$$I = \int_{\theta=0}^{2\pi} \int_{\ell=0}^{\ell_o} \ell \, d\ell \, d\theta \int_{\phi=0}^{2\pi} \int_{r=0}^{r_o} \frac{r \, dr \, d\phi}{b^2 + \ell^2 + r^2 - 2r\ell \cos(\theta - \phi)}. \tag{V-9}$$

Now consider the monitor foil. It is of the same area and same position relative to the dural plate as the disc source; therefore, the total number of fissions induced by neutrons scattered in the dural plate is given by an expression similar to Eq. (V-5), i.e.,

$$N_m = \frac{q}{4\pi} \left(\frac{\rho t N \sigma_f}{A}\right)_m I \quad , \tag{V-10}$$

where I is defined by Eq. (V-9) and the subscript m refers to the monitor foil. The total numoer of fissions in the monitor foil from direct neutrons is given by

$$N'_m = (nv)_{th} \, a\left(\frac{\rho t N \sigma_f}{A}\right)_m \quad , \tag{V-11}$$

- 39 -

and the ratio of fissions caused by scattered neutrons to fissions caused by direct neutrons is:

$$\frac{N_m}{N'_m} = \frac{\left(\dfrac{\rho t N \sigma_s}{A}\right)_{Al} I}{4\pi a} . \tag{V-12}$$

Now, the total number of fissions in the disc source, obtained from Eq. (V-8), is

$$N_{TU} = N'_U \left\{ 1 + \frac{\left(\dfrac{\rho t N \sigma_f}{A}\right) I}{4\pi a \left[1 - \left(\dfrac{\rho t N \sigma_t}{A}\right)_{Al}\right]} \right\} \tag{V-13}$$

or

$$N_{TU} = N'_U \left(1 + \delta_U\right). \tag{V-14}$$

where δ_U is substituted for the second term in the bracket. Similarly, the total number of fissions in the monitor foil, obtained from Eq. (V-12), is

$$N_{Tm} = N'_m \left[1 + \frac{\left(\dfrac{\rho t N \sigma_s}{A}\right)_{Al} I}{4\pi a} \right] \tag{V-15}$$

or

$$N_{Tm} = N'_m \left(1 + \delta_m\right). \, . \tag{V-16}$$

Now, the ratio of the number of fissions in the disc source to the number of fissions in the monitor foil, obtained from Eqs. (V-14) and (V-16), is

$$\frac{N_{TU}}{N_{Tm}} = \left(\frac{N'_U}{N'_m}\right)\left(\frac{1 + \delta_U}{1 + \delta_m}\right) . \tag{V-17}$$

From Eqs. (V-7) and (V-11)

$$\frac{N'_U}{N'_m} = \frac{(nv)_{th}\, a \left(\dfrac{\rho t N \sigma_f}{A}\right)_U \left[1 - \left(\dfrac{\rho t N \sigma_t}{A}\right)_{Al}\right]}{(nv)_{th}\, a \left(\dfrac{\rho t N \sigma_f}{A}\right)_m}$$

- 40 -

or

$$\frac{N'_U}{N'_m} = \frac{M_U}{M_m} \left[1 - \left(\frac{\rho t N \sigma_t}{A}\right)_{Al} \right] , \tag{V-18}$$

where M_U and M_m are the uranium masses of the disc source and monitor foil, respectively. Substituting Eq. (V-18) into Eq. (V-17), we have

$$\frac{N_{TU}}{N_{Tm}} = \frac{M_U}{M_m} \left[1 - \left(\frac{\rho t N \sigma_t}{A}\right)_{Al} \right] \left(\frac{1 + \delta_U}{1 + \delta_m}\right) . \tag{V-19}$$

It remains now only to evaluate δ_U and δ_m, or, in particular, to evaluate I. If in Eq. (V-9), we carry out in a straightforward manner the integrations over r and ϕ, we obtain

$$I = \int_{\theta=0}^{2\pi} \int_{\ell=0}^{\ell_o} \ell \, d\ell \, d\theta \, \ln \left\{ \frac{\sqrt{(b^2 + r_o^2 + \ell^2)^2 - 4r_o^2 \ell^2} + r_o^2 + b^2 - \ell^2}{2b^2} \right\} \tag{V-20}$$

Integration over θ reduces Eq. (V-20) to

$$I = -2\pi \int_{\ell=0}^{\ell_o} \ell \, d\ell \, \ln \left\{ \frac{\sqrt{(b^2 + r_o^2 + \ell^2)^2 - 4r_o^2 \ell^2} + r_o^2 + b^2 - \ell^2}{2b^2} \right\} . \tag{V-21}$$

Now we note that for this experiment, $b^2 = 0.00098$ in.^{2}, $r_o^2 = 0.1914$ in.^{2}, i.e., $b^2 << r_o^2$. Using this in Eq. (V-21), we find that the integral becomes:

$$I = 2\pi \int_{\ell=0}^{\ell_o} \ell \, d\ell \, \ln 2$$

or

$$I = \pi \left(\ln 2 \right) \ell_o^2 . \tag{V-22}$$

Substituting Eq. (V-22) into the expressions for δ_U and δ_m, we obtain

$$\delta_U = \frac{\left(\frac{\rho t N \sigma_s}{A}\right)_{Al} \left(\ln 2 \right) \ell_o^2}{4a \left[1 - \left(\frac{\rho t N \sigma_t}{A}\right)_{Al} \right]} \tag{V-23}$$

$$\delta_m = \frac{\left(\frac{\rho t N \sigma_s}{A}\right)_{Al} \left(\ln 2\right) \ell_o^2}{4a} \tag{V-24}$$

Evaluating δ_U and δ_m by substituting into Eqs. (V-22) and (V-23) the proper numbers for this experiment, we obtain

$$\left.\begin{aligned} \delta_U &= 0.781 \left(10^{-2}\right) \\[2mm] \delta_m &= 0.775 \left(10^{-2}\right) \end{aligned}\right\} \tag{V-25}$$

Similarly

$$\left[1 - \left(\frac{\rho t N \sigma_t}{A}\right)_{Al}\right] = 0.9914. \tag{V-26}$$

Substituting Eqs. (V-25) and (V-26) into Eq. (V-19), we obtain

$$\frac{N_{TU}}{N_{Tm}} = (0.992) \frac{M_U}{M_m}$$

This correction is taken into account in determining the cross sections given in Table 1.

APPENDIX VI

FISSION FRAGMENT LOSS IN THE HEMISPHERICAL URANIUM DEPOSITS

In the case of most of the U^{235} monitor foils, the uranium deposit was thin and a negligible number of fragments did not escape from the uranium. However, in order to give a satisfactory fission rate, the U^{238} deposits were heavier. Integral bias curves (plateaus) were taken of these fissions. An extrapolation of these plateaus to zero bias was used to account for those fragments that escaped from the uranium even though with an appreciable energy loss.

The following analysis is used to determine the fraction of the fission events for which the fragments did not escape from the uranium and so could not be accounted for by the plateau. We are considering a hemispherical deposit of uranium which gives equal probability of fission at all depths in the deposit. For simplicity we consider all fragments to have the same range in uranium. Take r_1 as the inner radius and r_2 as the outer radius of the deposit. The radial distance from the inner surface to the point of fission is taken as x. The distance of the fragment through the uranium to the point of escape at the outside of the hemisphere is taken as t where the angle between the fragment direction and the radial extension from the hemisphere is θ. By the law of cosines, the geometric relation between these quantities is simply

$$r_2^2 = (r_1 + x)^2 + t^2 - 2(r_1 + x)\, \ell \cos(\pi - \theta),$$

or

$$t = -(r_1 + x) \cos \theta + \sqrt{r_2^2 - (r_1 + x)^2 \sin^2\theta}\ . \tag{VI-1}$$

If we take N as the number of fissions produced per unit radial depth in the uranium, then the total produced per elemental depth dx is Ndx. Further, the total number F_L of fragments that do not escape from the uranium is

$$F_L = \int_{x=0}^{x = x_{max}} dx\; N \cos \left[\theta_o(x) \right]\ , \tag{VI-2}$$

where x_{max} is the uranium depth above which value all fragments escape from the hemisphere and $\theta_o(x)$ is the angle of the fragment direction above which value the fragments do not escape.

The depth of the complete escape x_{max} is found simply from $t_m = 10^{-3}$ cm, which is roughly the range of fragments in U_3O_8, by

$$(r_1 + x_m)^2 + (10^{-3})^2 = r_2^2,$$

where $r_1 = 7.65$ cm and $r_2 = r_1 + 10^{-5}$ cm (here 10^{-5} is the total depth of the uranium deposit). From this we obtain the value $x_m = 19.9(10^{-6})$cm. Similarly, the complete escape angle $\theta_0(x)$ applying to fissions from the partial escape depths is found from

$$r_2^2 = (r_1 + x)^2 + t_m^2 + 2(r_1 + x) t_m \cos \left[\theta_0(x) \right] . \qquad \text{(VI-3)}$$

Substitution of the experimental values in Eq. (VI-3) gives

$$\cos \left[\theta_0(x) \right] = \frac{(10^{-5} - x)(15.24 + 10^{-5} + x) - 10^{-6}}{2(7.62 + x)(10^{-3})} . \qquad \text{(VI-4)}$$

The number of fissions lost F_L is now found by substituting Eq. (VI-4) and $x_m = 9.9(10^{-6})$ into Eq. (VI-2). For the $\sim 10^{-5}$ cm thickness of U^{238} deposits used we obtain the value $F_L = 4.9(10^{-8})N$. However, the total number of fissions in this deposit is $F_t = 10^{-5}N$. Combining these values, we find that the percentage of fissions that do not escape from the uranium deposit is $F_L/F_t = 0.7\%$. This value has been used in calculating the final results given in Table 1.